

INELASTIC SCATTERING OF γ RAYS ON Ag^{107}

O. V. BOGDANKEVICH, B. S. DOLBILKIN, L. E. LAZAREVA, and F. A. NIKOLAEV

P. N. Lebedev Physics Institute, Academy of Sciences, U.S.S.R.

Submitted to JETP editor April 13, 1963

J. Exptl. Theoret. Phys. (U.S.S.R.) **45**, 882-891 (October, 1963)

The $\text{Ag}^{107}(\gamma, \gamma')\text{Ag}^{107m}$ yield was measured in the 30-MeV synchrotron of the Physics Institute by the induced activity method, with E_γ max varying from 6 to 26 MeV. The cross section calculated from the yield curve has one peak near the (γ, n) threshold and another in the 18–24 MeV region. The peak cross section values are 1.7 and 2.9 mb, respectively, with half-widths of approximately 4 MeV. The ratio of the cross section for inelastic γ -ray scattering by Ag^{107} to the photoneutron cross section σ_n [sum of the cross sections for the reactions $\text{Ag}^{107}(\gamma, n) + \text{Ag}^{107}(\gamma, 2n) + \text{Ag}^{107}(\gamma, pn)$] in the region of the first maximum agrees satisfactorily with the statistical theory. For the second maximum the ratio $\sigma(\gamma, \gamma')/\sigma_n$ exceeds the calculation by several orders of magnitude.

THERE has been very little investigation of inelastic γ -ray scattering on nuclei. The inelastic photon scattering cross section has been measured for only the four nuclei Y^{89} ,^[1] Rh^{103} ,^[2] In^{115} ,^[3] and Au^{197} ^[4] in the range 5–25 MeV. All data were obtained by the method of induced activity, i.e., by measuring the number of isomers of the initial stable isotope that were formed in the reaction $(Z, A) \rightarrow (\gamma, \gamma') \rightarrow (Z, A)^m$. This method requires the following conditions: (1) stable isotopes must have metastable states whose half-lives can be recorded; (2) there must be no neighboring isotopes that can form the same isomer through other possible reactions such as (γ, n) , $(\gamma, 2n)$, (γ, p) , etc.; (3) it must be possible to isolate the activity associated with a given isomer against the background of total induced activity in the sample. All these requirements are satisfied for only a few elements, so that the method has very limited application.

The utilization of the method can be considerably expanded by using samples consisting of separated isotopes. In the present work we have used silver samples enriched to from 94 to 98.5% Ag^{107} . Induced activity was used to measure the cross section of the reaction $\text{Ag}^{107}(\gamma, \gamma')\text{Ag}^{107m}$ in the range 6–26 MeV. The work was done at the 30-MeV synchrotron of the Lebedev Physics Institute.¹⁾

MEASUREMENT TECHNIQUE

A natural mixture of silver isotopes contains 51.35% of the mass-107 isotope and 48.65% of the

mass-109 isotope. When Ag^{107} and Ag^{109} are irradiated with 26-MeV γ rays induced activity results from the reactions listed in Table I. Both stable silver isotopes are seen to have isomeric states with very close half-lives (44 sec for Ag^{107m} and 40 sec for Ag^{109m}) and approximately equal metastable energy levels (93.5 and 87.7 keV, respectively). It is practically impossible to separate the yields of these isomers when registering the induced activities of samples. For example, if a sample contains both silver isotopes, we can measure only the sum of the cross sections for the reactions $\text{Ag}^{107}(\gamma, \gamma')\text{Ag}^{107m}$ and $\text{Ag}^{109}(\gamma, \gamma')\text{Ag}^{109m}$.

Above 16 MeV, Ag^{107m} is also formed in the reaction $\text{Ag}^{109}(\gamma, 2n)\text{Ag}^{107m}$. The inelastic scattering cross section can be measured by the induced activity method at energies above the threshold of this reaction in principle only if a separated isotope is used. Since the enriched samples contained only a few percent of the 109-isotope, parallel measurements were obtained from samples enriched in Ag^{107} and from samples of natural silver. This enabled us to determine the activity associated with Ag^{107} alone.

Among the product-nuclei formed in the photo-disintegration of Ag^{107} almost the same half-lives as that of Ag^{107} are exhibited by the isomers Pd^{105m} and Rh^{105m} formed in (γ, np) and $(\gamma, 2p)$ reactions. Because of the ~ 10 -MeV Coulomb barrier these reactions have an appreciable yield beginning at $E_\gamma \sim 20$ MeV and 24–25 MeV, respectively.^[8] It will be seen subsequently that as a result of the chosen technique the activities of these isomers remained practically unregistered.

¹⁾Preliminary results appeared in [5].

Table I

Reaction	Ag^{107}						Ag^{109}					
	Thresh- old,* MeV	Product nucleus	Type of decay	Half- life	Emission energy MeV		Thresh- old, *MeV	Product nucleus	Type of decay	Half- life	Emission energy MeV	
					Of particles	Of γ rays					Of particles	Of γ rays
(γ, γ')	—	Ag^{107m}	IT	44 sec	—	0.0935	—	Ag^{109m}	IT	40 sec	—	0.0877
(γ, n)	9.4	Ag^{106} Ag^{106}	β^+ (63%) EC (37%) β^- (1%) EC	24 min 8.3 days	β^+ : 1.96; 1.45 β^- : 0.5 —	— 0.5 0.220	9.2	Ag^{108}	β^- : 98.5% EC: 1.5%	2.3 min	1.5	>0.4
$(\gamma, 2n)$	17.8	Ag^{105}	EC	~ 40 days	—	0.064 >0.150	16.4	Ag^{107m}	IT	44 sec	—	0.0935
(γ, np)	15.2	Pd^{105m}	IT	~ 23 sec	—	0.20	15.5	Pd^{107}	β^-	$\sim 7 \times 10^6$ yr	~0.04	—
$(\gamma, 2p)$	14.8	Rh^{105} Rh^{105m}	β^- IT	36.5 hr 45 sec	0.570 (86%) 0.210 (4%) —	0.320 0.130	16.6	Rh^{107}	β^-	~ 25 min	1.2	—
(γ, α)	2.4	Rh^{103m}	IT	56min	—	0.040	2.9	Rh^{105} Rh^{105m}	β^- IT	36.5 hr 45 sec	0.570 (96%) 0.210 (4%) —	0.320 0.130

*The (γ, n) reaction thresholds were taken from [6]; the others were taken from Cameron's table in [7]; IT — isomeric transition; EC — electron capture.

The number of isomeric nuclei Ag^{107m} and Ag^{109m} formed during the irradiation was measured by registering with scintillation counters the γ quanta emitted in transitions from the metastable to the ground state. Despite the large internal conversion coefficients (20.3 for Ag^{107m} [9] and 22.4 for Ag^{109m} [10]) this procedure was more efficient than the registration of soft conversion electrons, because considerably thicker samples could be used. In addition, the introduction of corrections for absorption and scattering of the investigated radiation is simplified. The geometric dimensions, weight, and isotopic composition of the enriched samples are given in Table II. Similar samples of natural silver were prepared.

The measurements were performed with two different counting setups for the ranges 6–13 MeV and 11–26 MeV. The yield curves were matched at 11–13 MeV.

Table II

Sam- ple	% of Ag^{107}	% of Ag^{109}	Wgt., g	Thick- ness, μ	Area, mm
1	94.6	5.4	5.60	530	50 × 21
2	97.14	2.86	6.38	604	50 × 21
3	97.14	2.86	6.31	597	50 × 21
4	98.5	1.5	1.84	174	50 × 21
5	98.5	1.5	1.63	154	50 × 21
6	98.5	1.5	1.88	178	50 × 21

At energies below and somewhat above the (γ, n) reaction threshold practically all activity of the samples was associated with the formation of Ag^{107m} and Ag^{109m} . Therefore the principal requirement with regard to the counting apparatus was maximum registration efficiency with a relatively small counter background.

Figure 1 is a block diagram of the apparatus used for measurements in the 6–13-MeV range. The silver samples were irradiated for 2 minutes in a photon beam from the synchrotron. When the beam was cut off the samples were lowered (in a vertical "lift") to a scintillation counter located below at a distance ~ 1 m. Registration of the induced activity began 5 sec after the termination of the irradiation. In order to minimize the photomultiplier noise background, each crystal was placed in optical contact with two FÉU-1S photomultipliers connected in coincidence.

In order to reduce the cosmic ray background as well as the background from activity induced by photoneutrons and γ rays scattered in the counter during the irradiation period, the crystals and photomultipliers were shielded by 10–15 cm of lead and 30–50 cm of paraffin. The crystals were also surrounded by a 3–4 cm boron carbide layer. The counter background was also reduced by a factor of 4.5–5 by pulse-height analysis.

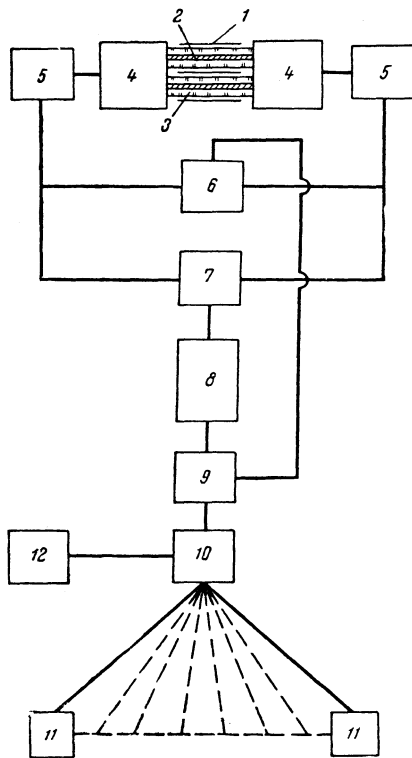


FIG. 1. Block diagram of apparatus for measurements in the range $E_{\gamma_{\max}} = 6 - 13$ MeV. 1—samples; 2— $22 \times 32 \times 2.5$ mm crystals; 3—light pipes; 4—photomultipliers FÉU-1S; 5—pre-amplifiers; 6—coincidence circuit; 7—summator; 8—amplifier; 9—single-channel pulse-height analyzer; 10—20-channel time delay selector; 11—mechanical register; 12—relay trigger circuit.

The decay curves of induced activity were measured automatically with a 20-channel time delay selector having an 8-second channel width, connected to follow the amplitude analyzer. The electronic circuit controlled the length of the irradiation period, the lowering of the sample to the counter, and the triggering of the time delay analyzer.

Measurements in the 11–26 MeV region required primarily the reliable discrimination of $\text{Ag}^{107\text{m}}$ and $\text{Ag}^{109\text{m}}$ activities against an appreciable activity background of other radioactive isotopes, especially Ag^{106} and Ag^{108} , formed during the irradiation period. In this case the counting efficiency played a smaller part, since the yield from $\text{Ag}^{107}(\gamma, \gamma')\text{Ag}^{107\text{m}}$ in the given energy region is considerably higher.

For measurements in the 11–26 MeV range we used alternately the enriched samples Nos. 4, 5, and 6, in which the Ag^{109} content was only one-half of that in Nos. 1, 2, and 3. The irradiation time was reduced to 45 sec, in order to decrease the relative yield of activities having longer half-lives.

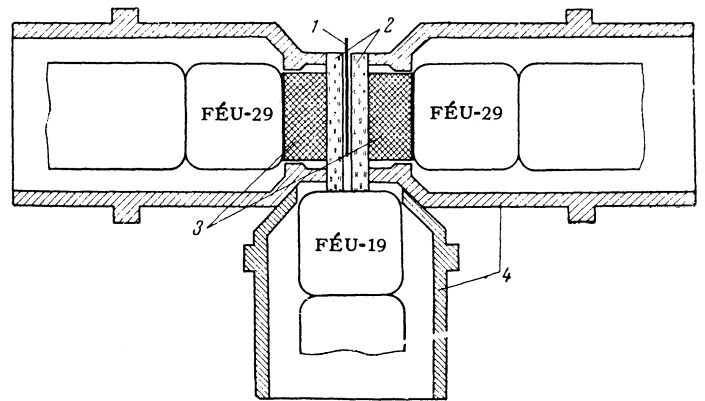


FIG. 2. Arrangement of samples and detectors for registering activity induced in samples by photons with $E_{\gamma_{\max}} > 13$ MeV. 1—Ag sample; 2—plastic scintillators; 3—NaI(Tl) crystals; 4—magnet shielding.

The detector is represented schematically in Fig. 2. Gamma rays representing isomeric transitions of $\text{Ag}^{107\text{m}}$ and $\text{Ag}^{109\text{m}}$ were registered with two counters consisting of NaI(Tl) crystals (30 mm in diameter and 15 mm thick) and FÉU-29 photomultipliers. Between the samples and the NaI(Tl) crystals there were positioned thin $55 \times 40 \times 7$ mm plastic scintillators of a third counter connected in anticoincidence with the main counters. This third counter absorbed less than 10% of the 90-keV photons passing through it, and excluded from registration the charged particles proceeding from the sample toward the NaI(Tl) crystals. The use of the scintillators of the third counter simply as absorbers resulted in a considerably smaller effect, since the predominant portion of β^- transitions of the radioactive background was accompanied by γ radiation, and the β^+ transitions were accompanied by annihilation radiation; both types of radiation were registered by the main counters.

The pulses from the main counters were fed to a common amplifier input, passed through the single-channel amplitude analyzer and the anticoincidence circuit, and were then fed to the 20-channel time delay selector. The first 160-second portion of the decay curve was measured with an 8-sec channel width; the selector was then triggered with a 32-sec channel width. A semilogarithmic curve was plotted, and the yields of activities having different half-lives were discriminated by the conventional graphical method.

The accuracy of the amplitude analyzer energy window was monitored regularly with a Tu^{170} source ($h\nu = 84$ keV). The window was 25 keV, corresponding approximately to the half-width of the distribution. This narrow window was re-

quired to exclude the registration of 200- and 130-keV γ rays accompanying the decays of $\text{Pd}^{105\text{m}}$ and $\text{Rh}^{105\text{m}}$ formed in the reactions $\text{Ag}^{107}(\gamma, \text{pn})$ and $\text{Ag}^{107}(\gamma, 2\text{p})$ at energies $E_{\gamma\text{max}}$ that were larger than ~ 20 and $24\text{--}25$ MeV, respectively (Table I). At the given amplitude resolution and chosen energy window, pulses of 200-keV photons (from $\text{Pd}^{105\text{m}}$) were completely cut off. Not more than 3–5% of pulses due to 130-keV photons were transmitted by the analyzer; thus practically no $\text{Rh}^{105\text{m}}$ activity was registered.

The sensitivity of the apparatus was checked regularly with a standard Tu^{170} source. The absolute efficiency for 90-keV γ rays was determined using a special Tu^{170} source in the form of a sample calibrated with $\pm 5\%$ accuracy.

The photon flux impinging on the sample was measured with a thick-walled (7.5 cm) aluminum ionization chamber, [11] which was positioned 25 cm beyond the sample during irradiation. The interior cross section of the chamber corresponded both in shape and in area to the "shadow" of the sample in the photon beam reaching this location from the synchrotron target. The energy of accelerated electrons was stabilized within ± 30 keV by the electronic circuitry.

During the irradiation of the silver sample, in addition to the (γ, γ') reaction metastable states of Ag^{107} and Ag^{109} could be excited through inelastic scattering of fast neutrons included in the accelerator background radiation, or of photoneutrons produced in the samples. In order to estimate the relative contributions of this process at $E_{\gamma\text{max}} = 25.5$ MeV, when this effect should reach its maximum, special control irradiations of the samples were performed. The usual irradiation conditions were changed; a 10-cm thick lead block was positioned in the beam path ahead of the sample; the fast neutron flux impinging on the sample was thus considerably enhanced. The results of these irradiations showed that the (n, n') reaction makes no appreciable contribution.

Both silver isotopes have a large cross section for slow-neutron capture. Since the slow-neutron background is approximately isotropic around the accelerator, we evaluated this effect by comparing the activities of samples placed at identical distances from the synchrotron both in and outside of the photon beam. Measurements at $E_{\gamma\text{max}} = 25$ MeV showed that with our registration technique the background of activity resulting from the reactions $\text{Ag}^{107}(n, \gamma)$ and $\text{Ag}^{109}(n, \gamma)$ was practically excluded.

YIELD CURVE AND CROSS SECTION FOR $\text{Ag}^{107}(\gamma, \gamma')\text{Ag}^{107\text{m}}$

Figure 3 shows the yields Y of the isomers $\text{Ag}^{107\text{m}}$ and $\text{Ag}^{109\text{m}}$ from samples enriched in Ag^{107} and from isotope mixtures, for maximum photon energies ranging from 6 to 26 MeV. The abscissa is $E_{\gamma\text{max}}$, and the ordinate is the number of isomeric $\text{Ag}^{107\text{m}}$ and $\text{Ag}^{109\text{m}}$ nuclei formed per second when one mole of silver was irradiated with the photon flux generating 1 A in the thick-walled aluminum chamber. Each experimental point is the average of from 20 to 100 irradiations. The rms errors are indicated.

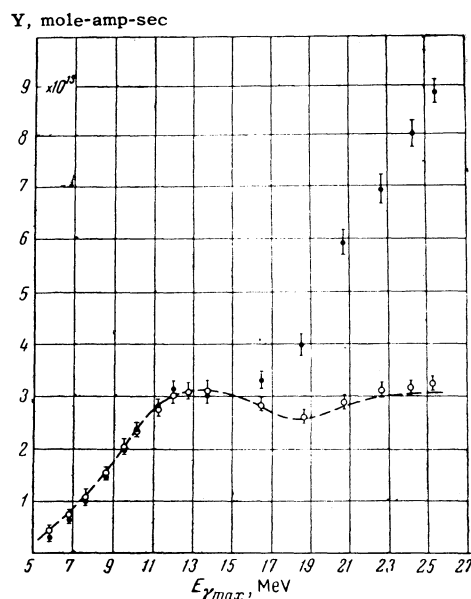


FIG. 3. Yields of $\text{Ag}^{107\text{m}}$ and $\text{Ag}^{109\text{m}}$ from enriched (O) and unenriched (\bullet) silver samples. The dashed curve represents the yield from the reaction $\text{Ag}^{107}(\gamma, \gamma')\text{Ag}^{107\text{m}}$.

At low energies up to about 15 MeV the yields from enriched and unenriched samples were identical within error limits. This means that in the range 6–15 MeV the cross sections for $\text{Ag}^{107}(\gamma, \gamma')\text{Ag}^{107\text{m}}$ and $\text{Ag}^{109}(\gamma, \gamma')\text{Ag}^{109\text{m}}$ are about equal. At larger energies, however, the results differ extremely. The sharp rise of the yield observed for the ordinary silver isotope mixture above $E_{\gamma\text{max}} \sim 17$ MeV should be associated primarily with the anticipated increase of the $\text{Ag}^{107\text{m}}$ yield from the $\text{Ag}^{109}(\gamma, 2\text{n})$ reaction with ~ 16.5 -MeV threshold.

A comparison of the data for the enriched and natural silver samples enables us to distinguish the effect associates with Ag^{107} alone for each given maximum photon energy.

The dashed curve represents the yield from $\text{Ag}^{107}(\gamma, \gamma')\text{Ag}^{107m}$. The cross section for this reaction calculated from the curve by the method given in [12] is shown in Fig. 4. Two cross section maxima are found at ~ 10 and ~ 21 MeV (1.7 and 2.9 b, respectively). The half-widths of the maxima are ~ 4 MeV.

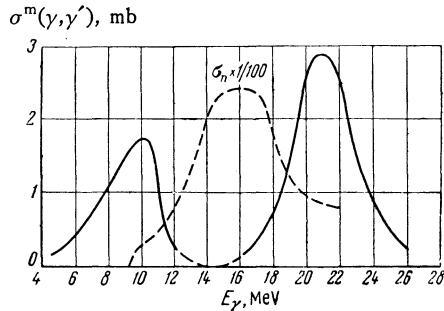


FIG. 4. Cross section for $\text{Ag}^{107}(\gamma, \gamma')\text{Ag}^{107m}$ compared with the (dashed) curve for the photoneutron cross section $\sigma_n \approx \sigma(\gamma, n) + \sigma(\gamma, 2n) + \sigma(\gamma, np)$ given in [13].

The figure also shows a curve of σ_n , representing the cross section sum $\sigma(\gamma, n) + \sigma(\gamma, 2n) + \sigma(\gamma, pn)$ measured for Ag^{107} in [13]. For medium and heavy nuclei in this energy region the sum of the cross sections for these reactions equals within a few percent the total cross section σ_γ for nuclear absorption of γ quanta. Figure 4 shows that the dipole resonance maximum at ~ 16 MeV coincides with the cross section minimum for $\text{Ag}^{107}(\gamma, \gamma')\text{Ag}^{107m}$. Thus the second peak for this reaction lies above giant resonance.

DISCUSSION OF RESULTS

The measured cross section for $\text{Ag}^{107}(\gamma, \gamma')\text{Ag}^{107m}$ comprises a fraction of the cross section for inelastic γ -ray scattering on Ag^{107} . To obtain the total inelastic cross section we must know the relative probability κ of isomeric state formation. It is impossible to perform any fairly accurate calculation of this quantity because the probability ratio of transitions from an excited state to the ground and metastable levels depends on the properties of all low-lying levels of the nucleus.

The available experimental data regarding the cross sections for the (γ, n) and $(\gamma, n)^m$ reactions leading to the ground and metastable states of the product nucleus [14] show that for each given nucleus the cross section ratio $\sigma(\gamma, n)/\sigma(\gamma, n)^m$ remains approximately constant from the (γ, n) threshold to ~ 25 MeV excitation energy. It can therefore be assumed that the measured cross section $\sigma(\gamma, \gamma')^m$ and the total inelastic scattering cross section $\sigma(\gamma, \gamma')$ in the 6–26-MeV range

exhibit more or less similar energy dependence.

According to the foregoing data the relative probability κ of transitions from an excited level of the initial nucleus to the metastable level of the final nucleus fluctuates in the range 0.2–0.8 in different cases. Similar values of κ are obtained by using the statistical weights of the spin states. [15] This means that the total inelastic scattering cross section may be several times larger than the measured cross section for $\text{Ag}^{107}(\gamma, \gamma')\text{Ag}^{107m}$.

As already mentioned, $\sigma(\gamma, \gamma')^m$ has a sharp maximum near the (γ, n) threshold, a relatively low value in the giant resonance region, and a second maximum in the region 18–24 MeV.

On the basis of the statistical model the inelastic scattering cross section is $\sigma(\gamma, \gamma') = \sigma_\gamma \Gamma_\gamma / \Gamma$, where σ_γ is the total absorption cross section, and Γ_γ and Γ are the radiation and total widths for a given excitation energy of the compound nucleus. As soon as the excitation energy exceeds the neutron binding energy, the neutron width Γ_n begins to increase very rapidly and the ratio Γ_γ / Γ diminishes sharply. If this decrease of the ratio is not compensated by a corresponding increase of σ_γ , then, beginning with the (γ, n) threshold, the inelastic scattering cross section must diminish drastically. Therefore the existence of the first maximum can be accounted for primarily by competition between radiative and neutron emission processes. Although the competition undoubtedly exists, the observed behavior of $\sigma(\gamma, \gamma')$ in the threshold region can also be associated with the existence of a maximum for the absorption cross section σ_γ , as follows from [16]. Analyzing the cross section maxima observed near the thresholds of the partial reactions (γ, n) and (γ, p) for elastic γ scattering on different nuclei, [17] Badalyan and Baz' have shown that both the absolute maximum of $\sigma(\gamma, \gamma')$ and the sharply varying parameters of this maximum that are observed in a comparison of different nuclei disagree with the statistical model. It is shown in both [16] and [18] that a qualitative explanation of the experimental findings is possible if it is hypothesized that photonuclear processes in the given energy range involve mainly a relatively small number of one-particle levels.

It is at present impossible in the given specific case to determine whether the first peak of the measured cross section $\sigma(\gamma, \gamma')$ results only from competition with the (γ, n) reaction or that the cross section for γ -ray absorption by Ag^{107} also possesses a maximum in this energy region. It is extremely interesting to investigate carefully, using a technique with high energy resolution, the

shape of the total cross section for γ -ray absorption at the thresholds of the partial reactions.

Figure 5 gives, for different excitation energies, the experimental ratios of $\sigma(\gamma, \gamma')^m$ and $\sigma_n \approx \sigma(\gamma, n) + \sigma(\gamma, 2n) + \sigma(\gamma, pn)$ obtained in the present work and in [13] (Fig. 4). The continuous curve represents the values of $\sigma(\gamma, \gamma')/\sigma_n$ calculated by one of the present authors, [19] using the statistical theory, from the ratio Γ_γ/Γ_n of the radiation and neutron widths.

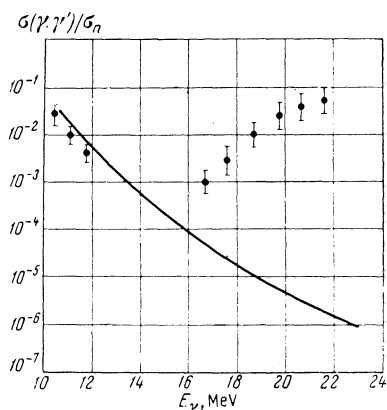


FIG. 5. Experimental ratios of $\sigma(\gamma, \gamma')^m$ and σ_n for different excitation energies. The curve was calculated on the statistical model.

At excitation energies a few MeV above the (γ, n) threshold photon emission is accompanied with high probability by neutron emission in the reaction $(\gamma, \gamma'n)$; therefore the ratio $\sigma(\gamma, \gamma')/\sigma_n$ should be smaller than Γ_γ/Γ_n . This was taken into account in the calculation in order to compute, in addition to the radiation width Γ_γ , the width $\Gamma_{2\gamma}$ corresponding to the successive emission of two γ quanta. The semi-empirical formula proposed by Newton [20] was used for the level density. The calculated curve gives the ratio of the total cross section for nuclear scattering proceeding via a compound nucleus to the photoneutron cross section σ_n [more precisely, the sum of $\sigma(\gamma, n)$ and $\sigma(\gamma, 2n)$ and the part of (γ, np) representing the prior emission of a neutron]. Since the measured value of $\sigma(\gamma, \gamma')^m$ is a part of this cross section, the calculated values can be several times larger.

Figure 5 shows that below 12 MeV theory and experiment are in qualitative agreement. This is entirely satisfactory considering the uncertain value of $\kappa\sigma(\gamma, \gamma')^m/\sigma(\gamma, \gamma')$ and the low accuracy of the calculation. Above 16 MeV the experimental results and the statistical theory calculation diverge sharply. At 20–22 MeV the experimental values are more than four orders larger than the theoretical results, indicating a very serious disagreement with the statistical theory.

The foregoing conclusion does not apply only to Ag^{107} . We also obtained anomalously large inelastic

scattering cross sections at 20 MeV for Rh^{103} [2] and In^{115} . [3] A large relative probability (~ 0.05) of radiative emission in the photodisintegration of carbon by 20–30 MeV photons is indicated in [21]. All these results suggest that inelastic scattering in this energy region is associated with some mechanism of interaction between γ rays and nuclei in which scattering plays an important part.

It is interesting to note that a similar picture is observed in the radiative capture of 14-MeV neutrons (the nuclear excitation energy being ~ 22 MeV). [22] The (n, γ) cross sections measured for a large number of nuclei exceed by a factor of 10^3 to 10^4 the cross sections calculated on the statistical theory. Satisfactory agreement between the experimental results reported in [22] and the theory was obtained in [23], where the mechanism of direct radiative capture was considered.

The foregoing discussion shows that further investigation of inelastic γ -ray scattering on nuclei is needed in the range $E_\gamma = 20$ –30 MeV.

The authors wish to thank electronics technician M. I. Sukhomyasov for his assistance in all stages of the experimental work, as well as the synchrotron crew headed by Engineer V. N. Logunov.

¹ E. Silva and J. Goldemberg, Phys. Rev. **110**, 1102 (1958).

² C. Sanchez del Río y Sierra and V. L. Telegdi, Phys. Rev. **90**, 439 (1953); Bogdankevich, Lazareva, and Moiseev, JETP **39**, 1224 (1960), Soviet Phys. JETP **12**, 853 (1961).

³ J. Goldemberg and L. Katz, Phys. Rev. **90**, 308 (1953); Burkhardt, Winhold, and Dupree, Phys. Rev. **100**, 199 (1955); Bogdankevich, Lazareva, and Nikolaev, JETP **31**, 405 (1956), Soviet Phys. JETP **4**, 320 (1957).

⁴ A. G. W. Cameron and L. Katz, Phys. Rev. **84**, 608 (1951); L. Meyer-Schützmeister and V. L. Telegdi, Phys. Rev. **104**, 185 (1956).

⁵ Bogdankevich, Dolbilkin, Lazareva, Moiseev, and Nikolaev, Proc. of the Rutherford Jubilee Intern. Conf., Manchester, 1961, Heywood, London, 1961, p. 833.

⁶ Geller, Halpern, and Muirhead, Phys. Rev. **118**, 1302 (1960).

⁷ A. G. W. Cameron, Atomic Energy of Canada Limited, AECL-433, 1958.

⁸ Ferrero, Hanson, Malvano, and Tribuno, Nuovo cimento **6**, 585 (1957); Kuo Ch'i-di and B. S. Ratner, JETP **39**, 1578 (1960), Soviet Phys. JETP **12**, 1098 (1961); Kuo Ch'i-di, Dissertation, Phys. Inst.

Acad. Sci. USSR, 1960; B. A. Yur'ev, JETP **43**, 1600 (1962), Soviet Phys. JETP **16**, 1127 (1963).

⁹ Brunner, Huber, Joly, and Maeder, Helv. Phys. Acta **26**, 588 (1953).

¹⁰ A. H. Wapstra and W. Van der Eijk, Nuclear Phys. **4**, 325 (1957).

¹¹ Flowers, Lawson, and Fossey, Proc. Phys. Soc. (London) **B65**, 286 (1952).

¹² A. S. Penfold and J. E. Leiss, Phys. Rev. **114**, 1332 (1959).

¹³ Bogdankevich, Goryachev, and Zapevalov, JETP **42**, 1502 (1962), Soviet Phys. JETP **15**, 1044 (1962).

¹⁴ Katz, Baker, and Montalbetti, Can. J. Phys. **31**, 250 (1953); Katz, Pease, and Moody, Can. J. Phys. **30**, 476 (1952).

¹⁵ Martin, Diven, and Taschek, Phys. Rev. **93**, 199 (1954).

¹⁶ A. M. Badalyan and A. I. Baz', JETP **40**, 549 (1961), Soviet Phys. JETP **13**, 383 (1961).

¹⁷ E. G. Fuller and E. Hayward, Phys. Rev. **101**, 692 (1956).

¹⁸ B. N. Kalinkin, JETP **36**, 1438 (1959), Soviet Phys. JETP **9**, 1022 (1959).

¹⁹ O. V. Bogdankevich, Dissertation, Phys. Inst. Acad. Sci. USSR, 1962.

²⁰ T. D. Newton, Can. J. Phys. **34**, 804 (1956).

²¹ Denisov, Kosareva, Tel'nov, and Cherenkov, Trans. 2nd All-Union Conf. on Nuclear Reactions at Low and Intermediate Energies, AN SSSR, Moscow, 1960, p. 1962.

²² Perkin, O'Connor, and Coleman, Proc. Phys. Soc. (London) **72**, 505 (1958).

²³ A. M. Lane and J. E. Lynn, Nuclear Phys. **11**, 646 (1959).

Translated by I. Emin

154